

CHARACTERIZATION OF NANOCRYSTALLINE AlTiSiN COATINGS DEPOSITED BY A LARC-CAE PROCESS

The paper presents the results of research studies involving the ceramic-metal tool materials with the deposited nitride coatings on the basis of aluminium, titanium and silicon. The cathodic arc evaporation with lateral rotating cathodes method was used for deposition of nanocrystalline, wear resistant nitride coatings – AlTiSiN type. Structural examinations are presented of the applied coatings and their support material made on the scanning electron microscope (SEM) and the scanning/transmission electron microscope (STEM). Chemical composition analysis as a function of the distance from the specimen surface, the so-called profile analysis, were carried out also. The structural analysis confirms that deposited multilayer coatings have dense microstructure without any visible porosity and delamination. It was found that the investigated coatings have nanocrystalline structure and consisting of fine crystallites even less than 6nm. Lattice deformations and numerous structural defects were also observed in the nanolayers. Depositing the AlTiSiN coatings results in the significant hardness increase within the range of 2252 ± 256 to 2908 ± 295 HV_{0.01}.

Keywords: AlTiSiN coatings, LARC-CAE process, Structural examinations

1. Introduction

In order to ensure high operational properties of modern tool materials, the top surface of tools should satisfy multiple characteristics: should have the desired structure and chemical composition, high hardness, a low friction factor and an appropriate thermal expansion coefficient in relation to the substrate material, low surface roughness and should exhibit stable properties together with the growth of working temperature. Advancements in the improvement of durability of tool materials have been achieved principally through the popularisation of deposition techniques of the hard coatings preventing the tool surface from premature wear. The deposition techniques of thin, hard coatings, which most often are the compounds of carbon, nitride, boron, oxide and transition metals, are so effective because a system of hard layers can be designed and fabricated having the desired properties, with a low chemical affinity to the material being worked, which are capable of transmitting substantial loads. Materials which form various types of coatings can be classified into three groups differing in the character of atomic bonds existing there, i.e. metallic, covalent or ion bonds. The materials which are forming coatings do not show pure bonds, but are characterised by mixed bonds with a complex combination of interactions: non-metal–non-metal, non-metal–metal, metal–metal, and their specific properties are conditioned by the type of the dominant atomic bond. None

of the material groups ensures that a coating is produced with universal properties, hence efforts have been constantly made to design appropriate chemical composition and a configuration of particular layers and to select their deposition method ensuring the required functional properties of tools designed for specific applications [1,2].

The tool materials based on the carbides of tungsten, titanium, tantalum, niobium and on a cobalt binding phase, covered with coatings which are based on the nitrides of transition metals such as Ti, Cr and Al – due to their high hardness, abrasion resistance and chemical stability – have been commonly used as tools for machining. The application of such coatings is limited, though, because of insufficient oxidation resistance at the temperature above 500°C, which usually occurs in high-speed machining [3-5].

Considering the numerous coating systems of transition metal nitrides, the research initiated by research institutions involved in surface engineering are focussed especially on multi-component coatings based on titanium, aluminium, chromium and silicon. TiAlSiN, AlTiSiN, CrAlSiN, AlCrTiN, AlCrSiN coatings, due to advantageous properties such as oxidation resistance and thermal stability at an elevated temperature, seem to fulfil the needs of protection of surfaces of high-speed cutting tools in difficult operating conditions [6,7].

The application of the fourth-generation nanostructured and/or graded coatings is considered to solve the problem of

* FACULTY OF MECHANICAL ENGINEERING, INSTITUTE OF ENGINEERING MATERIALS AND BIOMATERIALS, SILESIA UNIVERSITY OF TECHNOLOGY, AKADEMICKA 2A STR., 44-100 GLIWICE, POLAND

[#] Corresponding author: Anna.Tomiczek@polsl.pl

providing the numerous expected properties of wear-resistant coatings, not only in the coating-worked material contact zone, but also in the internal coating zone, and most of all in the transition zone between the coating and support material [8-12].

It cannot be clearly judged by analysing the usefulness of different PVD methods which of the coating deposition methods is definitely best. Physical vapour deposition methods, in particular the modified advanced methods of cathodic arc evaporation (e.g. CAE-LARC) [13-16] allow to deposit coatings consisting of nanolayers and with the nanometric grain size or a composite structure onto wear-resistant tool materials. Cathodic arc evaporation has been broadly employed for more than a decade for deposition of different types of wear-resistant coatings onto cutting tools which are characterised by high abrasion resistance and oxidation resistance at an elevated temperature or for applications where corrosion resistance is the key factor. Cathodic arc evaporation is distinct for a combination of many desired characteristics, e.g. a high deposition rate, high degree of ionisation (30-100%) and high energy of ions (20-120 eV) and consequently, the method is used extensively for surface layer modification. The strong adhesion of layers to the support material and mutually between particular interlayers is an indispensable condition in the majority of tribological applications. Another important advantage of cathodic arc evaporation is that several cathodes made of different materials are used in one chamber, and thus complex coatings are constituted having a diverse chemical composition.

The goal of this paper is to investigate the structure and selected properties of nanocrystalline, nanocomposite AlTiSiN coatings with the using the CAE-LARC method deposited on the ceramic-metal tool materials.

2. Material and methods

As a support material for CAE-LARC coating, a cemented carbide manufactured using powder injection moulding was used [16]. A modified method of cathodic arc evaporation with lateral rotating cathodes (Cathodic Arc Evaporation – Lateral Rotating Cathodes) on a device by PLATIT was applied for the deposition of nanocrystalline AlTiSiN coatings (Fig. 1). The device operates rotating cylindrical cathodes and their “universal” configuration offers high flexibility, permitting to achieve nanolayer, composite and nanocrystalline coatings.

A special arrangement of the layers forming part of the coatings is shown in Fig. 2. The layer deposition conditions were as follows: support material temperature of 400°C; working atmosphere of 100% N₂; the chamber pressure of 2 Pa. The specimens were, by default, cleaned chemically in washing and degreasing baths to prepare the surface directly before to the deposition of coatings. The specimens were then ion-etched in the chamber to activate the surface at an atomic scale.

The structure of the ceramic-metal tool materials with the deposited coatings was viewed in a ZEISS SUPRA 35 high-resolution scanning electron microscope at the accelerating

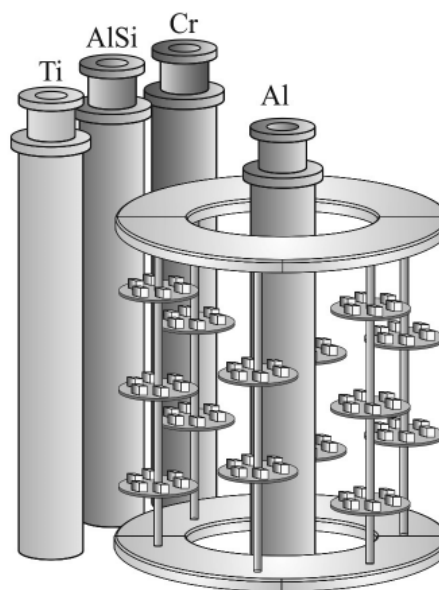


Fig. 1. The diagram of the cathodes distribution in the chamber of a PLATIT device

10 th layer AlTiSiN	Surface layer
9 th layer TiAlSiN	Multi-layers with varying chemical composition
8 th layer AlTiSiN	
7 th layer TiAlSiN	
6 th layer AlTiSiN	
5 th layer TiAlSiN	
4 th layer AlTiSiN	Gradient layer
3 rd layer TiAlSiN	
2 nd layer TiAlN/AlTiN	Adhesive sublayer
1 st layer TiN	
Cemented carbide	Support material

Fig. 2. Scheme of arrangement of the individual layers constituting the coating AlTiSiN marked on the tool materials

voltage of 10-20 kV, using back scattered electrons (BSE) and secondary electrons (SE) detection.

The structure and chemical composition were examined in a high-resolution transmission electron microscope S/TEM TITAN 80-300 by FEI, equipped with a STEM scanning system, BF, DF and HAADF scanning transmission detectors, a Cs condenser spherical aberration corrector, an electron energy filter, electron energy-loss spectrometer EELS, energy dispersion spectrometer. The value of accelerating voltage during measurements was 300 kV, and the observations were performed in the classical mode (TEM), with a spatial resolution of below 0.10 nm and in the scanning mode (STEM) with the spatial resolution of up to 0.14 nm. Thin foils from the support material and the deposited coatings were prepared with a FIB Quanta 3D 200i device, by thinning the initially cut lamellas to the thickness of 50-70 nm.

Two types of examinations were used in the S/TEM TITAN 80-300 microscope: with a parallel beam (TEM) and concentrated beam (STEM). By using a three-condenser setup, the size of the illuminated preparation surface was smoothly changed while maintaining the beam's parallelism. Diffraction images were obtained from an area with the diameter of not more than 200 nm, using Select-a-Shield (SAED) or from a region with the diameter of several or several dozens of nanometres without a shield (nanodiffraction).

The microhardness tests of coatings and support material were made on the DUH 202 SHIMADZU ultra microhardness tester.

Investigation of the friction coefficient and abrasion resistance of coatings to the substrates was determined using ball-on-plate test. Tribological tests performed on CSM Instruments tribometer equipped with a Taylor-Hobson Surtronic 25 profilometer under reciprocating motion with sinusoidal trajectory, with the following conditions: amplitude: 6 mm; maximum linear speed: 4.5 cm/s; load: 10 N; frequency: 2.9 Hz; counter-specimen: WC-Co/Al₂O₃ ball (diameter: 6 mm); distance: 500 m; ambient temperature: 25°C. The wear rate K of the Al,Ti,SiN coating can be calculated by the formula [17]:

$$K = V/F \cdot S$$

V – wear volume [mm³]; F – load [N]; S – sliding distance [m].

3. Results

It was found in metallographic examinations of lateral microsections and fractures made in a scanning electron microscope that an AlTiSiN coatings deposited on a support material made of ceramic-metal tool materials is characterised by a layered arrangement (Fig. 3a). Several layers with coatings having a different thickness and chemical composition, depending on the distance to the support material, were identified, which was confirmed in examinations with a high-resolution electron

transmission microscope. Spectral examinations with an X-ray energy-dispersive spectrometer confirm that the coatings deposited contain Al, Ti, Si, and N (Fig. 3b). Several layers of complex nitride AlTiSiN with a varying chemical composition and different thickness exist between the first layer of TiN deposited onto the support material and the outer AlTiSiN layer. The total thickness of AlTiSiN coatings was 2.8-3.0 mm. Regardless the situation, all the layers forming part of the composition tightly adhere to each other and do not show any fractures and discontinuities. In addition, fractographic tests of tool materials with the deposited AlTiSiN coatings do not reveal delamination along the separation area between the coating and the substrate, which indicates good adhesion of the coatings obtained on the support material of tools materials.

The coatings fabricated with the cathodic arc evaporation method with lateral rotating cathodes, composed of several layers, were characterised on the basis of examinations in an electron transmission microscope, and transition zones were examined between the support material and the individual layers. Figure 4 show images obtained in the scanning-transmission mode, with BF detectors. It can be concluded based on the examinations of thin foils from the cross-section of AlTiSiN nitride coatings deposited on the substrate of ceramic-metal tool materials, that they have a nanocrystalline and nanocomposite structure within the entire volume. AlTiSiN coatings do not show any discontinuities, fractures and porosity and feature a high homogeneity and a compact structure.

The existence of several layers (zones) in nitride layers was identified, based on aluminium, titanium and silicon, exhibiting a varying thickness and chemical composition depending on the distance from the substrate. A 180 nm thick TiAlN/AlTiN (2nd) layer, deposited directly onto a near-the-core TiN layer, showing a gradient character with a linearly decreasing concentration of titanium, at the same time with the growing concentration of aluminium (Fig. 5) and eight layers with a varying chemical composition and different thickness, was observed between the adhesive sublayer deposited on the substrate – 70 nm thick tita-

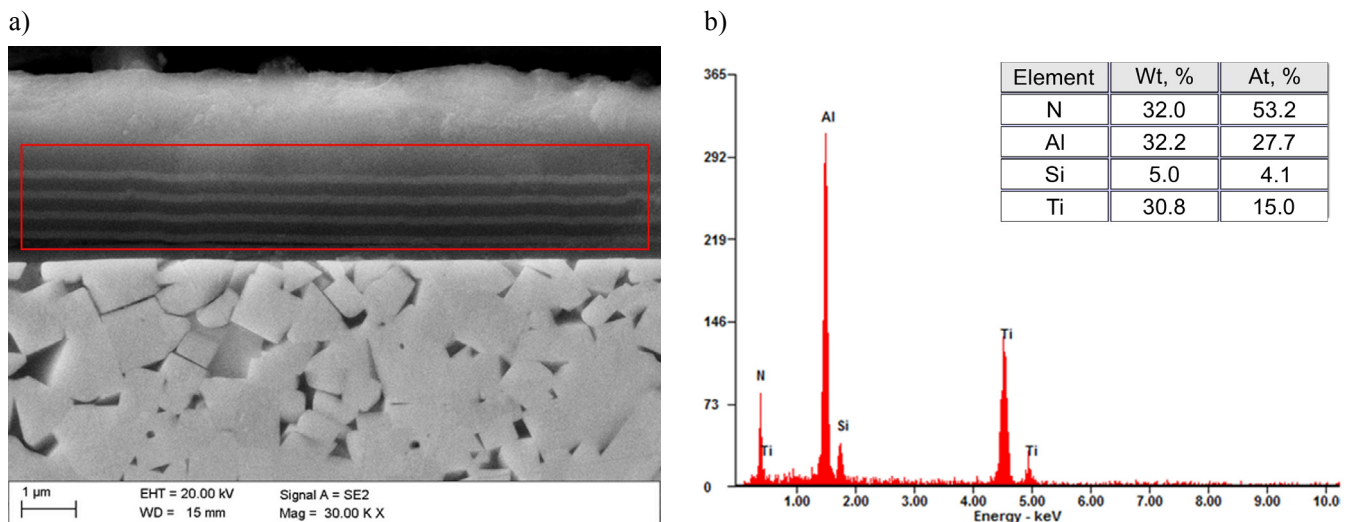


Fig. 3. Structure of AlTiSiN coating, SEM (a) and results of spectral examinations with an X-ray energy-dispersive spectrometer (b)

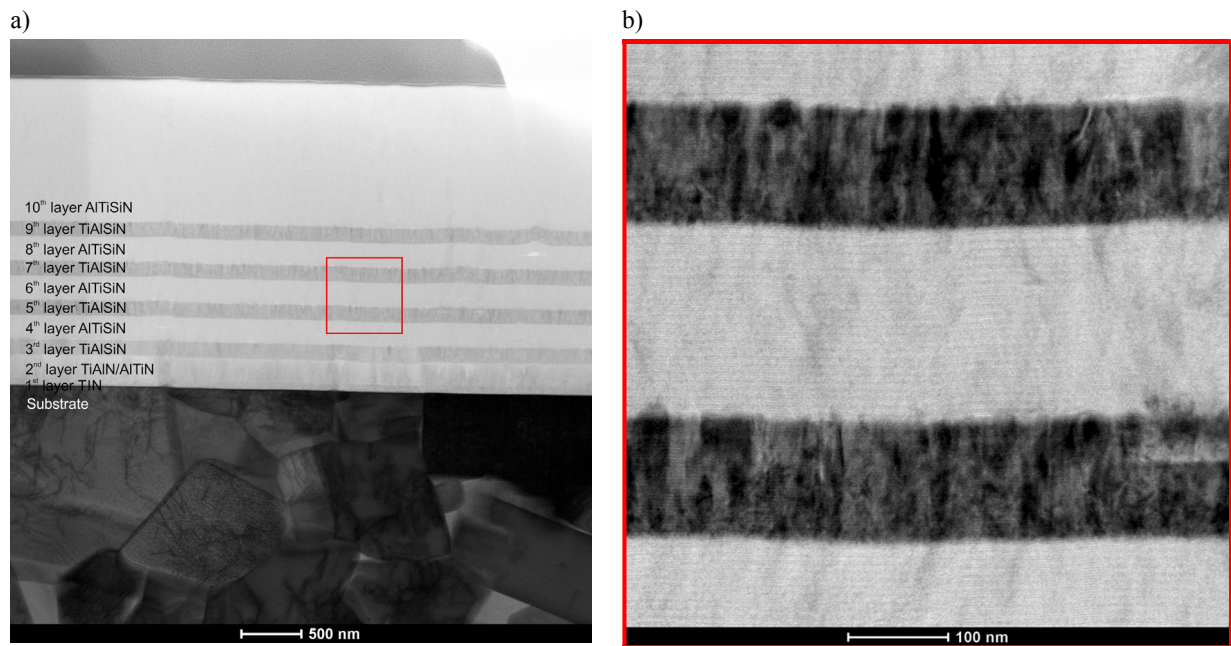


Fig. 4. Structure of multilayer AlTiSiN coating, BF S-TEM mode

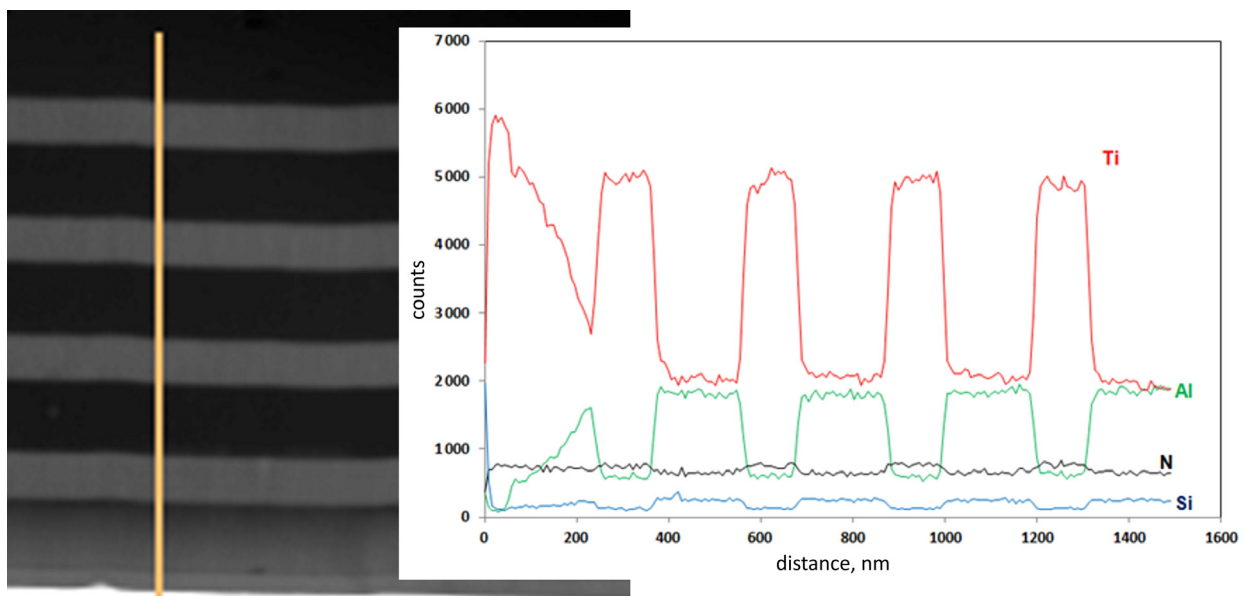


Fig. 5. Linear analysis of elements distribution on AlTiSiN multi-layer made with the energy-dispersion spectrometer

niium nitride (1st), and the outer AlTiSiN 1150 nm thick surface layer (10th). The thickness and chemical composition is changing alternately in the 3rd – 9th layers and is, respectively, 120 nm for a TiAlSiN layer and 200 nm for an AlTiSiN layer.

A linear analysis was carried out and a surface analysis of distribution of elements (Fig. 6) with the energy-dispersion spectrometer was performed to confirm that variations exist in the chemical composition of the particular layers (from 1st to 10th) of the AlTiSiN coating. The character of variations in the concentration of elements points out that particular layers exist. A sharp transition between a layer composed of titanium nitride and a substrate made of tool material was not noticed, either.

A lower concentration of elements originating from the coating was found in this place, along with an increased concentration of elements forming part of the substrate. This signifies that a diffusive transition layer exists, as confirmed in examinations with spectroscopic methods. A layer deposited directly onto a substrate, and a graded layer (respectively, 1st and 2nd) have a nanocrystalline structure. This is shown in BF and DF photos made in the transmission mode and in electron diffraction patterns (SADP, nanodiffraction), in HRTEM images and in their Fourier FFT transforms (Fig. 7).

A detailed analysis of the entire AlTiSiN coating reveals the presence of a nanolayer (Al+Si)TiN/Ti(Al+Si)N configuration parallel to the substrate with modulation (periodicity) of about

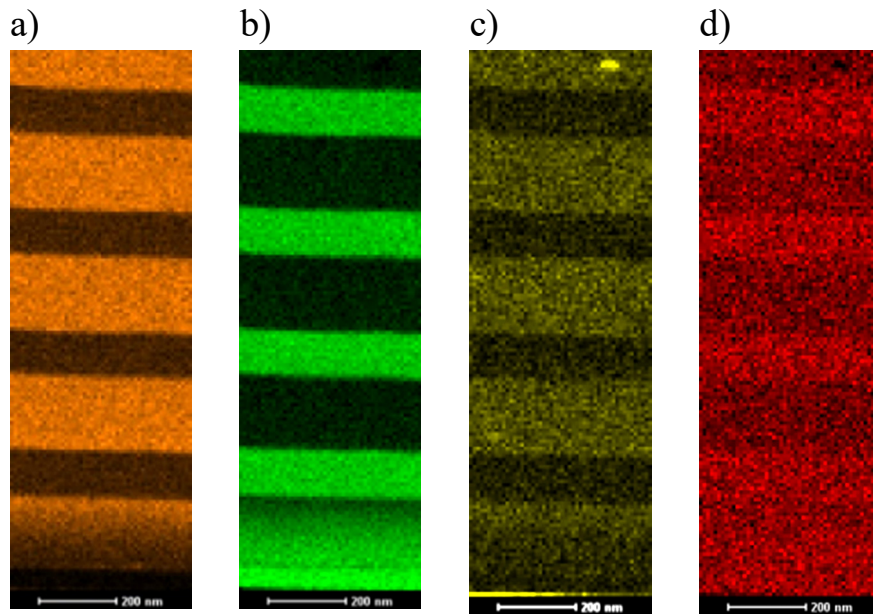


Fig. 6. Surface analysis of elements distribution made with the energy-dispersion spectrometer: a) Al, b) Ti, c) Si, d) N

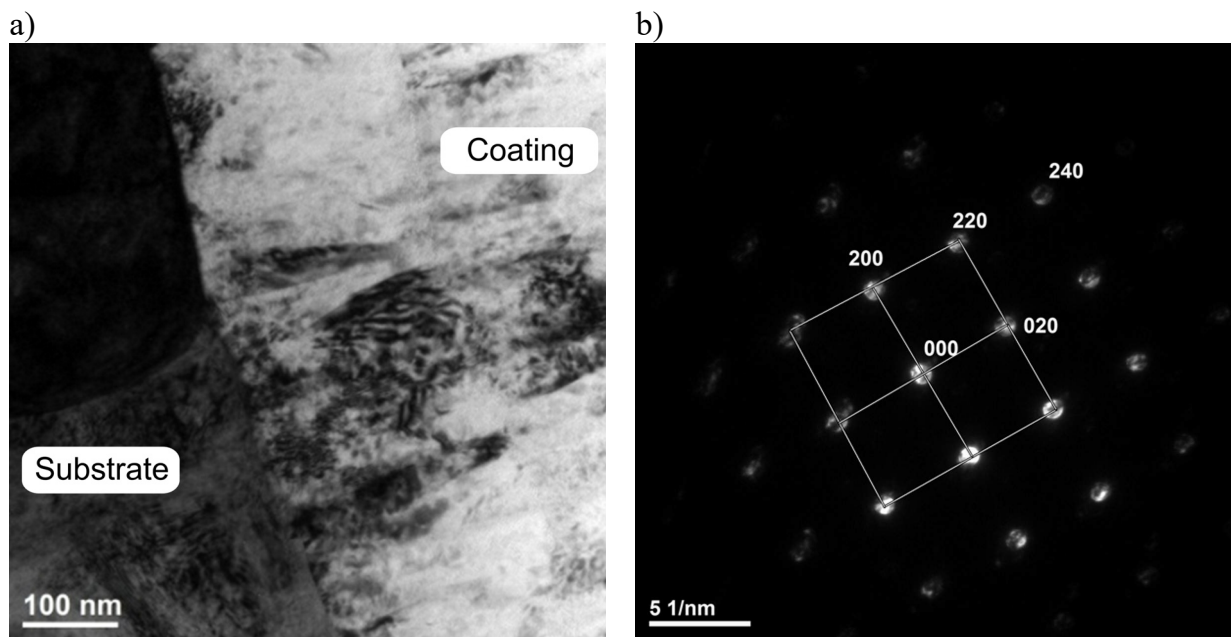


Fig. 7. Structure of the substrate/coating interface, TEM BF (a) and nanodiffraction (b)

3 nm. A distinctive lamination exists in the layers with a high concentration of titanium and with a column structure (1st, 2nd, 3rd, 5th, 7th, 9th), as well as in layers with a high concentration of aluminium (4th, 6th, 8th), and in a surface layer (10th), as illustrated in Fig. 4 and Fig. 8. The contrast observed is probably caused by a difference in the chemical composition of nanolayers and results from a different electrons scattering coefficient by Ti and Al atoms. The nanolayers rich in aluminium are brighter than those rich in titanium due to a lower scattering coefficient of Al [4,8].

A change in the chemical composition between nanolayers is caused by the character of coatings' deposition in a modified method of cathodic arc evaporation – LARC. Rotating cylindrical

cathodes are situated inside the chamber (in particular Ti and Al+Si) used for the deposition of complex coatings. The rate of changes is so high that a sharp transition is not observed between the particular nanolayers. The periodicity (~3 nm) of the nanolayers can be modulated and depends on the rotational speed of the mechanism. Strong lattice deformations and numerous structural defects, e.g. dislocations (Fig. 9) were found in the structure of the layers.

The contrast observed (Fig. 10) – caused locally by a different concentration of aluminium and titanium in grains (a higher concentration of aluminium) and around the grains (higher concentration of silicon) – may indicate a high level of stresses [18].

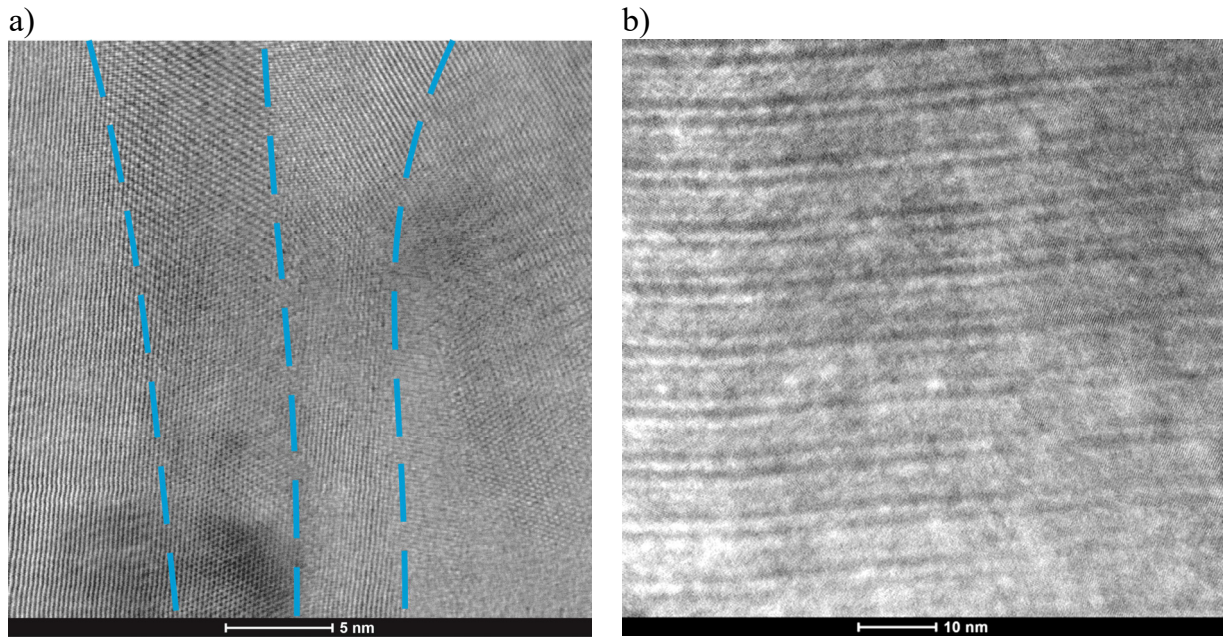


Fig. 8. The column structure of TiN (1st) layer, STEM, HAADF (a) and lamination structure of AlTiSiN (4th) layer, STEM, HAADF (b)

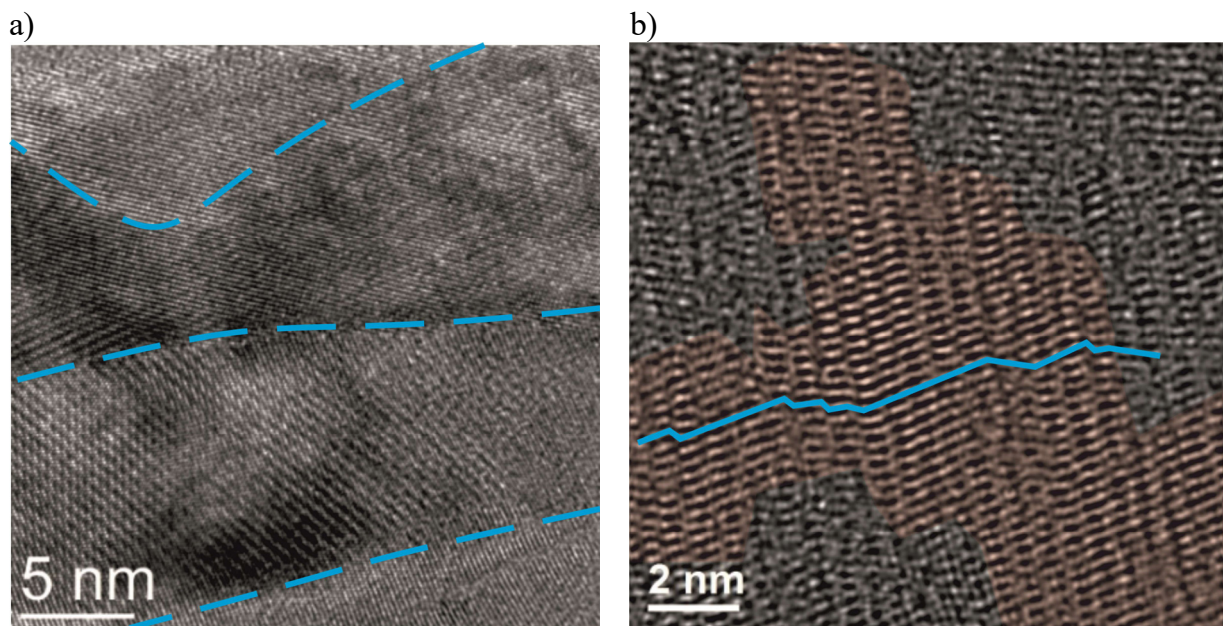


Fig. 9. Structure of TiAlSiN (3rd) layer (a) and AlTiSiN (6th) layer, HRTEM

Structural observations and diffraction images using imaging in the HRTEM mode and the corresponding Fourier FFT transforms confirm that the nitride coatings produced based on aluminium, titanium and silicon exhibit a nanocrystalline and nanocomposite structure.

It was found that the microhardness of the uncoated ceramic-metal tool materials was 1497 ± 108 to 1711 ± 158 HV_{0.01}. Depositing the AlTiSiN coatings onto the substrate results in the significant surface hardness increase within the range of 2252 ± 256 to 2908 ± 295 HV_{0.01}. No relationship was found between the substrate hardness and hardness of the deposited surface layer – these results were confirmed by ball-on-plate tribology test.

The test results confirm the validity of the tribological materials for the manufacture of tool wear-resistance of coatings by physical vapour deposition as nanocrystalline, nanocomposite AlTiSiN coatings are characterised by superior wear-resistance of ceramic-metal tool materials. Basing on the analysis of wear track profiles made after the tribological tests (the distance of 500 m), it was found that the maximum depth of wear is smaller than the thickness of the coatings AlTiSiN, suggesting the absence of their total of wear. Cross-section profiles of wear track of the tested samples and wear rate K prove that the AlTiSiN coatings have much higher wear-resistance than the support material (Table 1).

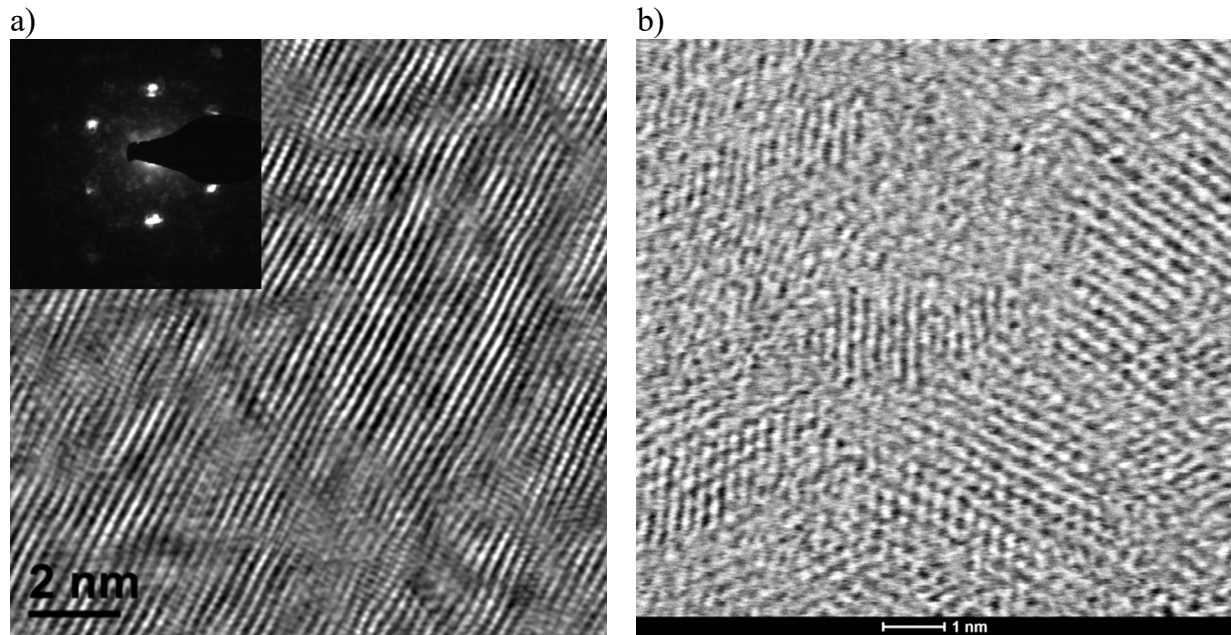


Fig. 10. Structure of AlTiSiN (6th) layer, HRTEM (a); STEM BF (b)

TABLE 1

Results of tribological test

Material	Friction coefficient, m	Wear rate K , mm ³ /Nm
Cemented carbide (support material)	0.69	20.9×10^{-6}
AlTiSiN coating	0.60	5.11×10^{-6}

4. Discussion

It was found based on the investigations and analyses undertaken that the use of injection moulded and sintered ceramic-metal tool materials with the deposited nanocrystalline and nanocomposite nitride coatings based on, aluminium, titanium and silicone, ensures almost a 5-fold growth of service life as compared to uncoated tools, and a nearly 3.5-fold growth as compared to TiAlN-coated tools [14]. An improvement in the operational properties of ceramic-metal tool materials, achieved through the deposition of AlTiSiN coatings produced with the CAE LARC method, should be linked to the enrichment of their chemical composition by adding aluminium creating nanostructured coatings and influencing the improved mechanical and tribological properties, including microhardness, corrosive resistance and, most of all, oxidation resistance and higher thermal stability at an elevated temperature [11,16,19,20]. An addition of silicone with a concentration of 3-6% increases microhardness and thermal stability as well as oxidation resistance, by creating amorphous or crystalline SiN_x with a high concentration of silicone along the boundaries of grains [21], and has also a substantial impact on the grain size by reducing, notably, the size of columns during layer growth, as confirmed by examina-

tions with a high-resolution electron microscope. The structure of a coating and a special composition of the layers forming the coating, has undoubtedly influence on high functional properties. Diversity in the deposition of hard nitrides enables to create any composition of individual layers, especially to use a layer with the graded character (2nd layer) and layers exhibiting nanocrystalline and nanocomposite structure (3rd-10th). Numerous works [9,10,22,23] prove that the size of nanocrystalline grains should range between 3 and 10 nm, separated with 1-2 nm areas of the amorphous phase for crystalline areas with a high concentration of silicon (for AlTiSiN coatings).

5. Conclusions

Deposited by cathodic arc evaporation with lateral rotating cathodes AlTiSiN coating has been investigated in detail as to their nanocrystalline and nanocomposite structure. The dense microstructure of the multilayer coatings without any visible porosity and delamination was observed in the scanning electron microscope. HRTEM investigation shows AlTiSiN layers with column structure and fine crystallites, while their size is even less than 6 nm. However, strong lattice deformations and numerous structural defects, have been observed using HRTEM investigation.

It was found that the depositing the AlTiSiN coatings results in the significant hardness increase within the range of 2252 ± 256 to 2908 ± 295 HV_{0.01}. Moreover, cross-section profiles of wear track of the tested samples and wear rate K prove that the AlTiSiN coatings have much higher wear-resistance than the cemented carbide used as support material.

Acknowledgements

This work was supported by the Ministry of Science and Higher Education of Poland as the statutory financial grant of the Faculty of Mechanical Engineering, Silesian University of Technology.

REFERENCES

- [1] S. Zhang (Ed.), *Handbook of Nanostructured Thin Films and Coatings*, CRC Press, Taylor and Francis Group (2010).
- [2] B. Tlili, C. Nouveau, M.J. Walock, M. Nasri, T. Ghrib, *Vacuum* **86**, 1048-1056 (2012).
- [3] Y.Y. Chang, C.P. Chang, D.Y. Wang, S.M. Yang, W. Wu, *J. Alloys Compd.* **461**, 336-341 (2008).
- [4] M. Parlinska-Wojtan, A. Karimi, T. Cselle, M. Morstein, *Surf. Coat. Technol.* **177-178**, 376-381 (2004).
- [5] L. Aihua, D. Jiannxin, C. Haibing, C. Yangyang, Z. Jun, *Int. J. Refract. Met. H.* **31**, 82-88 (2012).
- [6] M. Stueber, H. Holleck, H. Leiste, K. Seemann, S. Ulrich, C. Ziebert, *J. Alloys Compd.* **483**, 321-333 (2009).
- [7] K. Bobzin, N. Bagcivan, N. Goebbels, K. Yilmaz, B.R. Hoehn, K. Michaelis, M. Hochmann, *Surf. Coat. Technol.* **204**, 1097-1101 (2009).
- [8] L.A. Dobrzański, M. Szindler, M. Pawlyta, M.M. Szindler, P. Boryło, B. Tomiczek, *Open Phys.* **14**, 159-165 (2016).
- [9] K. Gołombek, L.A. Dobrzański, M. Soković, *J. Mater. Process. Technol.* **157-158** 341-347 (2004).
- [10] K. Lukaszewicz, L.A. Dobrzański, G. Kokot, P. Ostachowski, *Vacuum* **86**, 2082-2088 (2012).
- [11] E. Torres, D. Ugues, Z. Brytan, M. Perucca, *J. Phys. D: Appl. Phys.* **42**, 105306 (2009).
- [12] K. Gołombek, G. Matula, J. Mikuła, M. Soković, *Mater. Technol.* **51** (1), 163-171 (2017).
- [13] L. Aihua, D. Jiannxin, C. Haibing, Ch. Yangyang, Y. Jun, *Int. J. Refract. Met. H.* **31**, 82-88 (2012).
- [14] C. Ducros, C. Cayron, F. Sanchette, *Surf. Coat. Technol.* **201**, 136-142 (2006).
- [15] S. Zhang, L. Wang, Q. Wang, M. Li, *Surf. Coat. Technol.* **214**, 160-167 (2013).
- [16] W.Y. Hoa, C.H. Hsu, C.W. Chena, D.Y. Wang, *Appl. Surf. Sci.* **257**, 3770-3775 (2011).
- [17] S. Veprek, R.F. Zhang, M.G.J. Veprek-Heijman, S.H. Sheng, A.S. Argon, *Surf. Coat. Technol.* **204**, 1898-1906 (2010).
- [18] L.A. Dobrzański, K. Gołombek, *J. Mater. Process. Technol.* **164-165**, 805-815 (2005).
- [19] J. Musil, *Surf. Coat. Technol.* **207**, 50-65 (2012).
- [20] F. Sanchette, C. Ducros, T. Schmitt, P. Steyer, A. Billard, *Surf. Coat. Technol.* **205**, 5444-5453 (2011).
- [21] M.G. Faga, G. Gautier, R. Calzavarini, M. Perucca, E. Aimo, F. Cartasegna, L. Settineri, *Wear* **263**, 1306-1314 (2007).
- [22] H.C. Barshilia, B. Deepthi, K.S. Rajam, *Vacuum* **81**, 479-488 (2006).
- [23] X.Z. Ding, X.T. Zeng, Y.C. Liu, *Thin Solid Films* **519** (6), 1894-1900 (2011).
- [24] T. Marten, B. Alling, E. Isaev, H. Lind, F. Tasnadi, L. Hultman, I. Abrikosov, *Phys. Rev. B* **85**, 104106 (2012).